1999 International Ash Utilization Symposium, Center for Applied Energy Research, University of Kentucky, Paper #69. Copyright is held by the Authors.
http://www.flyash.info

Reactions of Calcium and Sodium during Combustion of Lignite

A. D. Shah, G. P. Huffman*, F. E. Huggins, and N. Shah, CFFLS, 533 S. Limestone St., University of Kentucky, Lexington, KY 40506-0043
J. J. Helble, University of Connecticut, Storrs, CT
T. W. Peterson and J. Wendt, University of Arizona, Tucson, AZ
A. F. Sarofim, University of Utah, Salt Lake City, UT

Abstract
Calcium and sodium are abundant elements in low rank coals that can play a major role in ash fouling and slagging processes that result in reduced boiler efficiency during combustion. This paper presents an analytical investigation of the reactions of calcium and sodium during combustion of a lignite in two different combustion facilities. The principal analytical technique used in the study was computer-controlled scanning electron microscopy (CCSEM). Complementary data were obtained using x-ray absorption fine structure (XAFS) spectroscopy and Mössbauer spectroscopy. The reactions of calcium and sodium with clay minerals, quartz, and SO_2 are interpreted using ternary composition diagrams and particle size distributions (PSD) derived from the CCSEM analysis of the ash. It is found that Ca and Na may react either with aluminosilicates derived from clay minerals to form Ca- and Na- containing glass phases or with SO_2 to form Ca, Na and Ca-Na sulfates.

Introduction

The current paper is focused on the analytical results obtained from ash samples generated from Beulah lignite in combustion tests conducted at the University of Arizona (UA) and at the State Electricity Commission of Victoria (SECV) in Australia. Most of the results presented were obtained by computer-controlled scanning electron microscopy (CCSEM). However, x-ray absorption fine structure (XAFS) spectroscopy and Mössbauer spectroscopy results will also be discussed where appropriate.

Experimental Procedures

Combustion conditions:

The combustion experiments were carried out with utility grind coal in a 2-5 kg/hr down-flow, self-sustained combustor at the University of Arizona (UA) and a 35 kg/hr pilot scale combustion test facility at the State Electricity Commission of Victoria (SECV) in Australia. At UA, the samples were collected using an Anderson cascade impactor to segregate the ash particles by size. The samples examined in this study from UA were nominally divided into three size ranges: >9 μm (impactor 1 + cup); 3-9 μm (impactors 2 + 3 + 4); and <3 μm (impactors 5 + 6 + 7 + 8 + AF (after filter)). The ash samples

* Author to whom correspondence should be directed. Phone number – (606) 257-4027; FAX – (606) 257-7215; e-mail – cffls@pop.uky.edu

collected at SECV were collected with no size segregation from the combustion zone and horizontal duct using isokinetic probes and from the electrostatic precipitator. More detailed discussions of the combustion conditions are given elsewhere.[1-3]

The coal used in these experiments was a Beulah lignite. Table 1 contains the proximate and ultimate analyses of the coal and the chemical composition of its ash.

CCSEM Method for Coal: The CCSEM used in this investigation consisted of a Tracor Northern 5500 system interfaced to an ISI 100 scanning electron microscope. The data is transferred from the TN5500 to either personal computers or a VAX station 4000/60 computer for data storage and analysis.

The CCSEM method of coal minerals analysis, which was originally developed [4,5] over ten years ago and has been refined and enhanced continuously since [6-16], measures the areas of cross-section and the energy-dispersive x-ray spectra (EDX) of at least 1200 different mineral particles in a random, polished section of the coal embedded in epoxy and reduces the data to derive the overall mineralogy of the coal. In the SEM, the computer-controlled electron beam is stepped across the field-of-view in a relatively coarse grid (256x256) in order to locate mineral particles in the coal/epoxy matrix. The back-scattered electron intensity is used to discriminate between mineral particles and the background of coal maceral and epoxy mounting medium. Once a mineral particle is located, the grid spacing is greatly reduced (4096x4096) and the area of cross section of the particle is measured by extending eight diagonals through the center to the edge of the particle and summing the areas of the triangles so produced. The electron beam is then positioned at the center of the particle and an EDX spectrum is rapidly (~8 sec) collected which provides the chemical information used as a fingerprint to identify the mineral. After typically 1200 particles have been measured in this way, the information is then transferred to a second computer, a VAX station 4000/60, for reduction and analysis. In the current version of the CCSEM software, there are twenty-five individual mineral categories and fifteen mixed categories into which the EDX spectrum might fall. By analyzing at least 1200 particles in the coal section in this manner, a reasonably quantitative description of the coal mineralogy can be obtained. Additional information obtained in the Coal Minerals Analysis (CMA) is a semi-quantitative description of the size distribution of individual mineral categories and the overall mineral matter.

CCSEM techniques for ash samples: CCSEM techniques for ash and slag samples are similar to those for the coal, except that the particles are normally not embedded in epoxy but are mounted on Nucleopore (0.2 μm) filters by a process of filtration in triply-distilled acetone. The amount of material filtered is adjusted to give an optimum density of particles on the filter paper, which is judged through an optical microscope. Hence, the area that is measured is that which the particle extends normal to the electron beam and not a cross-sectional area. The volume of the particle is then estimated from the area measured.

Similar data reduction techniques are used as in CMA, but the sorting program is more generic and is based on the intensity of the energy-dispersive X-rays from the three most

abundant elements, rather than on specific phases. The program identifies particles in which a single element, two elements, or three elements are dominant and labels them accordingly. For example, calcium-containing aluminosilicate glasses could fall into one of the categories, Ca-Si-Al, Si-Ca-Al, Al-Si-Ca, etc. The most abundant element in the category is first, so on. Categories containing the same three elements are then grouped together in the tabular outputs.

A variety of graphical methods have been developed for presenting the chemical information in the CCSEM ash data more clearly. These include the use of binary, ternary, and volume percentage/number frequency – ternary diagrams. Any element or combination of elements can be chosen as the endpoints or vertices of these diagrams. The threshold for the sum of the three elements in a ternary is set by the user; normally 80% is the value chosen, and this value was used for all ternary diagrams in this paper. More detailed discussions of our methods of graphical representation of CCSEM data have been given elsewhere [10].

Results and discussion

The inorganic material in lignite consists of both discrete and molecularly dispersed species. As discussed in earlier publications,[7, 17, 18] XAFS spectroscopy indicates that the Ca cations in most lignite and subbituminous coals are molecularly dispersed and bound to the oxygen anions of carboxyl groups. This type of structure is probably also correct for Na, but it has not been directly confirmed. However, it is compatible with the XAFS spectra observed for K which has been inserted into lignite by ion-exchange.[18]

The discrete mineral phases in the Beulah lignite were examined by CCSEM and the results are summarized in Table 2. Pyrite, kaolinite, quartz and "mixed silicates" are the dominant discrete mineral phases. The "mixed" phases usually represent two or more mineral particles that are located close enough together in the sample that they all contribute to the EDX spectrum, making assignment to a particular mineral phase ambiguous. In the case of the mixed silicates, the chief chemical constituents are Si and Al, indicating that most of the mineral particles contributing to the EDX spectra for this category are kaolinite and quartz. The presence of several percent of gypsum and ferrous sulfate indicate that weathering oxidation of the coal has occurred during storage prior to the combustion tests.

CCSEM results for the ash products from the combustion tests at UA and SECV are presented in Table 3 and Figures 1-3. Since that the SEM used in these studies did not have a light element detector, oxygen was not detected in the EDX spectra. Nevertheless, it is highly likely that all of the phases detected in the ash are oxide or sulfate phases and we will refer to them as such in this discussion. Focusing first on the results in Table 3, it is seen that three ternary phases are dominant in the ash products from both combustion tests: Ca-aluminosilicate glass, Na-aluminosilicate glass and Ca-Na-sulfates. Additionally, there are several percent of unreacted silica (SiO_2), calcium oxide (CaO) and iron oxides present. Mossbauer spectroscopy indicates that magnetite is the dominant iron oxide in the UA ash, while both hematite and magnetite are present in the SECV ash. This suggests that the SECV combustion test was conducted under more oxidizing conditions.

The composition ranges and formation mechanisms of the three ternary phases are clarified by the use of ternary diagrams. Figure 1 shows the volume frequency - ternary composition plots for Ca-Si-Al ash particles from both the UA and SECV combustion tests. For the UA ash, the larger particles separated by the Anderson cascade impactor (Imp. 1 + cup) exhibited a broad range of composition (Figure 1a) representing the degree of reaction between CaO fume and aluminosilicate with approximately a 1:1 ratio of Si:Al, derived from kaolinite. Significant amounts of unreacted CaO, SiO_2, and aluminosilicate are also evident in the diagram. The smaller ash particles from the test (Imp. 5-8 + AF) exhibit a narrower range of composition for this phase, concentrated near the center of the diagram (Figure 1b). The ash particles in the Ca-Si-Al category from the SECV tests exhibited a broad range of composition from CaO to aluminosilicate (Figures 1c and 1d). Unreacted CaO, SiO_2 and aluminosilicate were more prevalent in the SECV ash.

Typical volume frequency - ternary composition plots for Na-Si-Al ash particles are shown in Figure 2. Nepheline ($NaAlSiO_4$), the Na-aluminosilicate phase reported earlier [2,9] for Beulah ash samples, was observed in all of the current samples. Na-aluminosilicates were much more abundant for the SECV ashes than for the UA ashes, and were in fact the most abundant species observed for the SECV specimens. As seen in Figure 2, the compositions were similar to those observed earlier, and were centered roughly around $NaAlSiO_4$.

Finally, significant amounts of Ca-Na-sulfates were observed in all samples (Figure 3). Samples from the SECV pilot scale tests were not size-segregated and samples collected from various regions of the combustor contained Ca-Na-sulfates that covered a broad composition range. As illustrated in Figure 3d, the CCSEM ternary diagram covered a range of compositions from CaO to $CaSO_4$ to mixed Ca-Na sulfate to nearly pure Na_2SO_4. For the size-segregated UA ash samples, the larger particles contained only a small amount of the Ca-Na-sulfate phase and compositions near $CaSO_4$ were dominant (Figure 3a). In contrast, the fine size and intermediate size particles from the UA test contained substantially more sulfates and mixed Na-Ca-sulfates were dominant (Figures 3b and 3c).

Finally, the Ca-Si-S phase that is substantial for the UA ash in Table 3 appears to be primarily unburnt or partially burnt char. Examination of the composition of this phase shows it to contain about 15-35% S, 15-35% Ca, 15-40% Si, 5-10% Na, 1-5% Fe, and minor amounts of other elements (carbon cannot be detected with the current x-ray detector). These compositions suggest that these coal particles have begun to burn, but are still intact; S, Ca, and Na have begun to form sulfate phases, and other minerals are still imbedded in the char.

Summary

Analytical results have been presented for ash samples derived from combustion tests on Beulah lignite in a 35 kg/hr furnace (SECV) and a 3k g/hr facility (UA). CCSEM was the principal analysis technique, with complimentary data from XAFS and Mössbauer

spectroscopy. Volume frequency-ternary composition diagrams from CCSEM data established that the Beulah ash products from the UA and SECV tests exhibited three principal phases: a Ca-aluminosilicate slag or glass; a Na-aluminosilicate phase with compositions centered around nepheline ($NaAlSiO_4$); and a Na-Ca-sulfate. The composition ranges of these phases were observed to become tighter as the particle sizes decreased. Na interacted more strongly with aluminosilicates in the SECV run, while exhibiting a stronger tendency for sulfate formation in the UA runs. For the UA runs, Ca-aluminosilicates were dominant in the larger ash particles (2.5-20 um), while Na-Ca-sulfates were the dominant phase in the small particle ash fraction (< 5.0 um). Na-aluminosilicate was the most abundant phase in all SECV ash samples. Mössbauer spectroscopy data indicated that combustion conditions were more oxidizing for the SECV test than for the UA test.

Acknowledgement: This research was supported by the U.S. Department of Energy under DOE contract No. DE-AC22-86PC90751.

References

1. J.J. Helble, S. Srinivasachar, G. Wilenski, A.A.Boni, S.G.Kang, K.A. Graham, A.F. Sarofim, J.M. Beer, N.B. Gallagher, L.E. Bool, T.W. Peterson, J.O.L. Wendt, N. Shah, A. Shah, F.E. Huggins, and G.P. Huffman, **Transformations of Inorganic Coal Constitutents in Combustion Systems**, Final Report under DOE Contract No. DE-AC22-86PC90751, November 1992.

2. J.J. Helble, S. Srinivasachar, A.A. Boni, S.G. Kang, K.A.Graham, A.F. Sarofim, J.M. Beer, N.B. Gallagher, L.E. Bool, T.W. Peterson, J.O.L. Wendt, N. Shah, F.E. Huggins, G.P. Huffman, "Mechanisms of Ash Evolution – A Fundamental Study: Part 1 – Low Rank Coals and the Role of Calcium," 209-228, Proc. EFC, 1992.

3. J.J. Helble, S. Srinivasachar, A.A. Boni, L.E. Bool, N.B. Gallagher, T.W. Peterson, J.O.L. Wendt, F.E. Huggins, N. Shah G.P. Huffman, K.A. Graham, A.F. Sarofim, and J.M. Beer, "Mechanisms of Ash Evolution – A Fundamental Study: Part 2 – Bituminous Coals and the Role of Iron and Potassium," 229-249, Proc. EFC, 1992.

4. R.J. Lee, F.E. Huggins, and G.P. Huffman, "Correlated Mossbauer-SEM Studies of Coal Mineralogy, in Scanning Electron Micrscopy/1973/I, pp. 561-568, SEM Inc., AMF O'Hare, Chicago, IL 60666, USA.

5. F.E. Huggins, D.A. Kosmack, G.P. Huffman, and R.J. Lee, "Coal Mineralogies by SEM Automatic Image Analysis," Scanning Electron Microscopy/1980/I, pp. 531-540, SEM, Inc., AMF O'Hare, Chicago, IL 60666, USA.

6. F.E. Huggins, G.P. Huffman, and R.J. Lee, "Scanning Electron Microscopy-Based Automatic Image Analysis (SEM-AIA) and Mossbauer Spectroscopy: Quantitative Characterization of Coal Minerals," ACS Symposium Series No. 205, pp. 239-258, Coal and Coal Products: Analytical Characterization Techniques, Ed., E.L. Fuller, Jr., American Chemical Society, 1982.

7. G.P. Huffman and F.E. Huggins, “Analysis of the Inorganic Constitutents in Low-Rank Coals,” ACS Symposium Series No. 264, pp. 159-174, Chemistry of Low-Rank Coals, Ed., H.H. Schobert, Amer. Chem. Soc., 1984.

8. G.P. Huffman, F.E. Huggins, R.A. Shoenberger, J.S. Walker, R.B. Greegor, and F.W. Lytle, *Fuel* **65**, 621-632 (1986).

9. G.P. Huffman, F.E. Huggins, and N. Shah, “Behavior of Basic Elements During Coal Combustion,” *Progress in Energy and Combustion Science*, **16**, #4, pp. 293-302 (1990).

10. N. Shah, G.P. Huffman, F.E. Huggins, and A. Shah, “Graphical Representation of CCSEM Data for Coal Minerals and Ash Particles,” pp. 179-190, Proc. EFC, 1992.

11. P. Gottleib, N. Agron-Olshina, and D.N. Sutherland, “The Characterization of Mineral Matter in Coal and Fly Ash,” pp. 135-146, Proc. EFC, 1992.

12. A.F. Reid, P. Gottlieb, K.J. MacDonald, and P.R. Miller, *Applied Mineralogy*, Metallurgical Society AIME, pp. 191-204 (1984).

13. E.N. Steadman, T.A. Erickson, B.C. Folkedahl, and D.W. Brekke, “Coal and Ash Characterization: Digital Image Analysis Applications,” pp. 147-164, Proc. EFC, 1992.

14. C.J. Zygarlicke and E.N. Steadman, *Scanning Electron Microscopy*, **4** (3), pp. 579-590 (1990).

15. W.E. Straszheim and R. Markuzewski, “Characterization of Mineral Matter in Coal for Prediction of Ash Composition and Particle Size,” pp. 165-177, Proc. EFC, 1992.

16. W.E. Straszheim and R. Markuzewski, *Energy & Fuels*, **4** (6), 748 (1990).

17. "An EXAFS Investigation of Calcium in Coal," F. E. Huggins, G. P. Huffman, F. W. Lytle, and R. B. Greegor, Proceedings of the 1983 International Conference on Coal Science, Pittsburgh, PA; pp. 679-682 (International Energy Agency, 1983).

18. A.D. Shah, G.P. Huffman, F.E. Huggins, N. Shah, and J.J. Helble, **1995**, *Fuel Processing Technology*, **44**, 105-120.

Table 1. Proximate, ultimate and ash analyses for Beulah lignite (wt. %).

Proximate	*As Received*	*Dry*	Ultimate	*As Received*	*Dry*	Ash Chemistry	Wt.% ash
Fixed carbon	30.9	44.2	Carbon	41.30	59.1	SiO_2	21.6
Vol. Matter	29.3	41.9	Hydrogen	2.92	4.18	Al_2O_3	14.5
Ash	9.65	13.8	Oxygen	13.84	19.8	Fe_2O_3	12.2
Moisture	30.2	--	Nitrogen	0.82	1.18	CaO	17.1
			Sulfur	1.31	1.88	MgO	4.2
						Na_2O	6.1
						K_2O	0.3
						SO_3	21.1

Table 2. CCSEM discrete mineral weight percentages for Beulah lignite (weight % mineral matter basis).

Mineral Species	Wt % Mineral Matter
Quartz	11
Kaolinite	20
Illite	2
Mixed Silicates	25
Pyrite	16
Ferrous Sulfate	3
Gypsum	10
Ca-rich (Calcite)	3
Miscellaneous Mixed	10

Table 3. CCSEM results (volume %) of the Beulah lignite ash samples from combustion test facilities at UA and SECV.

	UA Burn 48F				SECV	
Elemental Categories	**Imp 1+cup**	**Imp 2+3+4**	**Imp 5+6+7+8+AF**	**Comb. Chamber**	**Horiz. Duct**	**ESP**
Si	**5**	**-**	**-**	**4**	**2**	**1**
Ca	**4**	**-**	**-**	**7**	**5**	**5**
Fe	**2**	**-**	**-**	**4**	**2**	**3**
Si-Al	**-**	**-**	**-**	**2**	**1**	**1**
Ca-Si	**1**	**-**	**-**	**-**	**-**	**-**
Ca-S	**3**	**1**	**-**	**10**	**7**	**6**
Na-S	**-**	**-**	**-**	**-**	**-**	**1**
Na-Si	**1**	**-**	**-**	**1**	**2**	**1**
Ca-Si-Al	**36**	**16**	**5**	**15**	**12**	**11**
Na-Si-Al	**14**	**6**	**2**	**29**	**22**	**23**
Fe-Si-Al	**-**	**-**	**-**	**1**	**2**	**-**
K-Si-Al	**-**	**-**	**-**	**1**	**-**	**-**
Ca-Si-Na	**2**	**2**	**2**	**-**	**-**	**-**
Ca-Si-S	**12**	**31**	**13**	**3**	**3**	**4**
Na-Si-S	**-**	**-**	**3**	**-**	**1**	**3**
Ca-Na-S	**3**	**31**	**64**	**4**	**7**	**13**
Ca-Fe-S	**-**	**-**	**-**	**6**	**9**	**6**
Ca-Mg-S	**1**	**-**	**-**	**3**	**3**	**5**
Others	**17**	**13**	**11**	**11**	**22**	**17**

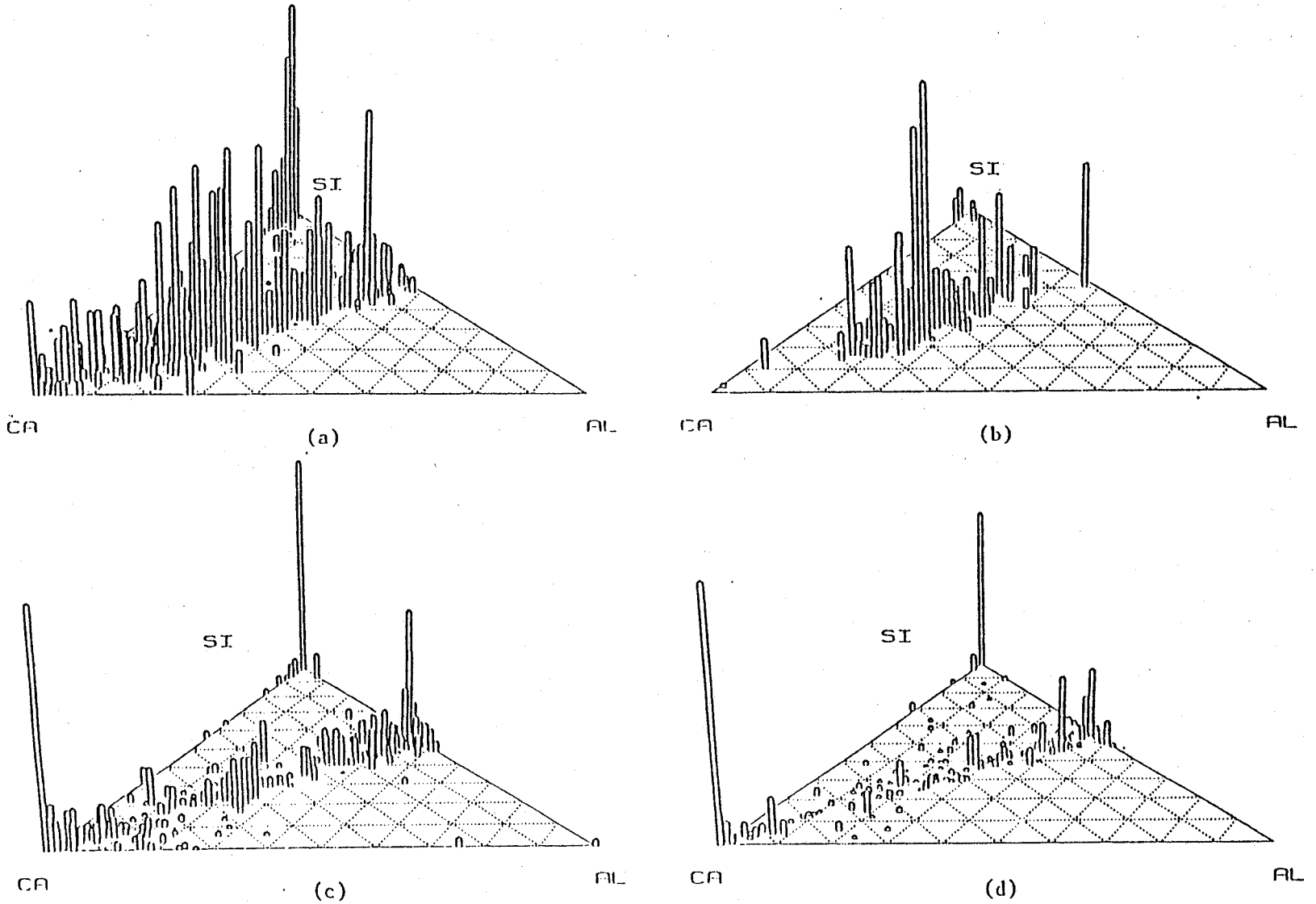

Figure 1. Ca-Si-Al volume frequency-ternary plots for Beulah lignite ash from: (a) UA combustor, Imp. 1 + cup; (b) UA combustor, Imp. 5-8 + AF; (c) SECV combustor, combustion chamber; and (d) SECV combustor, horizontal duct.

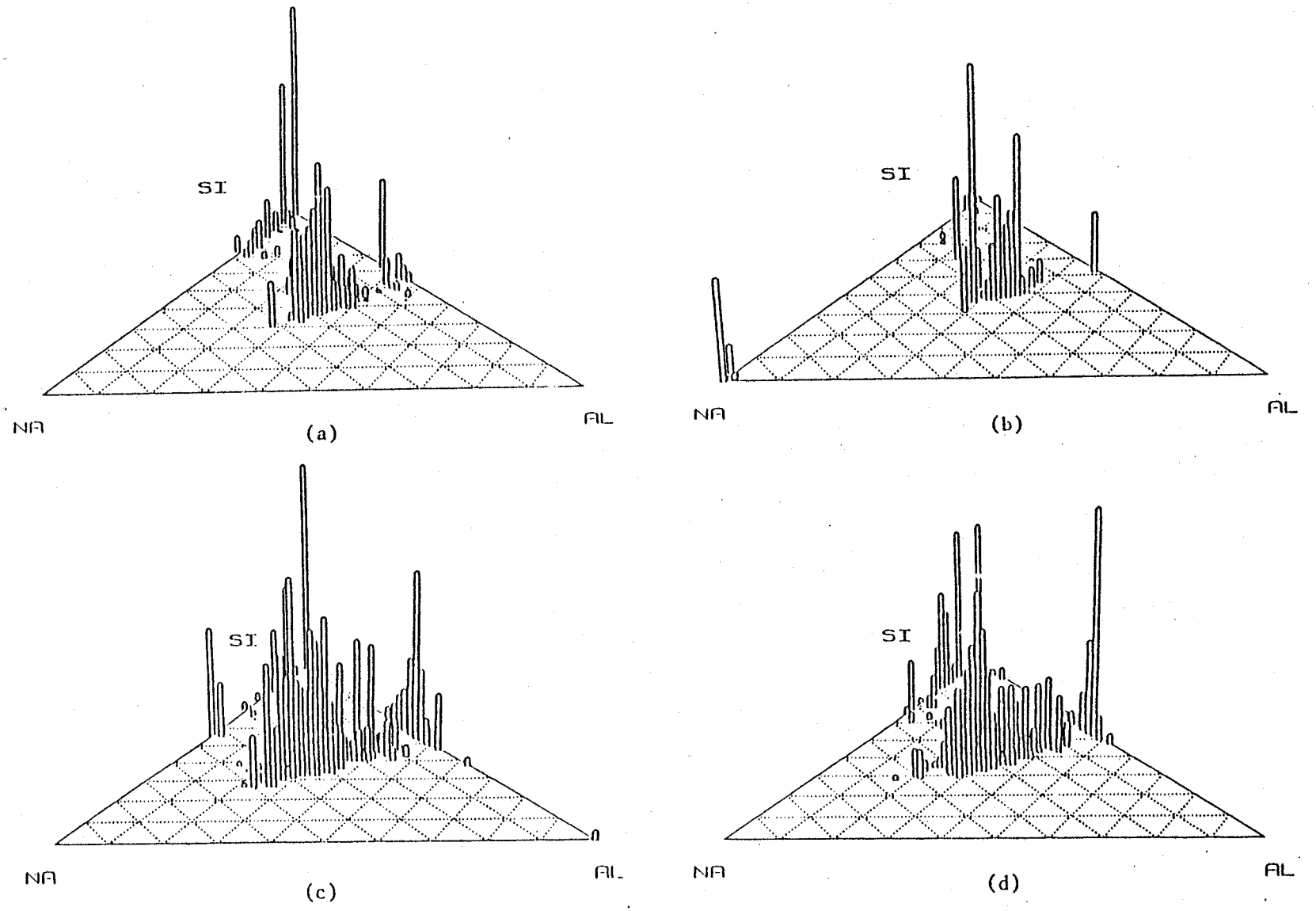

Figure 2. Na-Si-Al volume frequency-ternary plots for Beulah lignite ash from: (a) UA combustor, Imp. 1 + cup; (b) UA combustor, Imp. 5-8 + AF; (c) SECV combustor, combustion chamber; and (d) SECV combustor, horizontal duct.

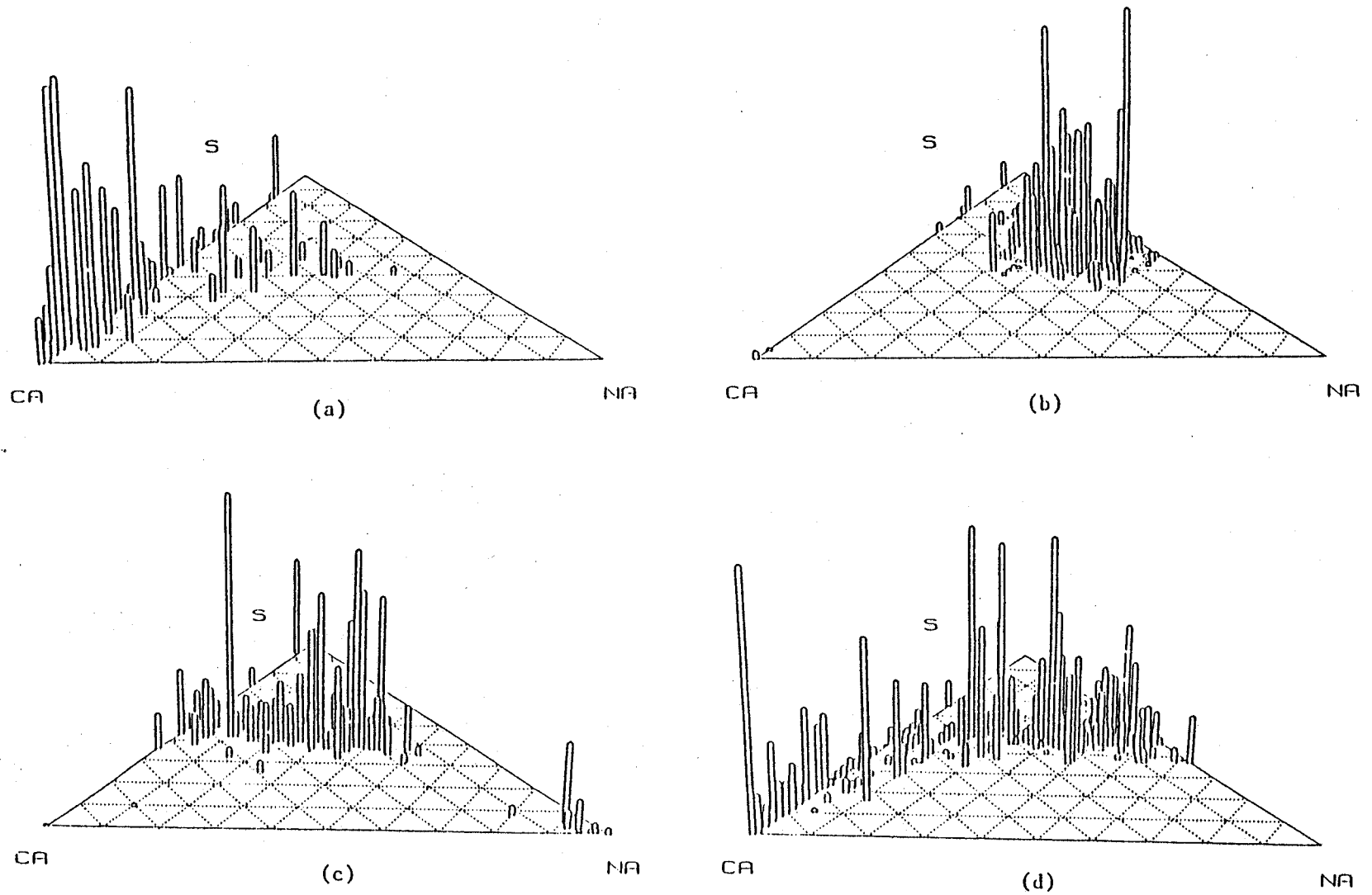

Figure 3. Ca-Na-S volume frequency-ternary plots for Beulah lignite ash from: (a) UA combustor, Imp. 1 + cup; (c) UA combustor, Imp. 2 + 3 + 4; (b) UA combustor, Imp. 5-8 + AF; and (d) SECV combustor, electrostatic precipitator.